




# The Temperature Stability of Nanometric Multilayers of Copper and Chromium–Nickel Steel (Cu/310S)

Barbara Kucharska<sup>1</sup> · Edyta Olejnik<sup>2</sup> 

Received: 22 September 2018 / Accepted: 5 March 2019 / Published online: 16 March 2019  
© The Author(s) 2019

## Abstract

Multilayers consisted of Cu and AISI 310S steel fabricated on a Si(100) monocrystalline silicon substrate by the magnetron sputtering method were investigated. The multilayers were differentiated by the number of periods (50, 100 and 150) and by the thickness of 310S steel sublayer (2 nm and 4 nm), while maintaining a constant thickness of the Cu (2 nm). The temperature stability tests were performed in an air atmosphere by isothermal annealing in the temperature range from 23 °C to 400 °C. It was found that the temperature stability of Cu/310S steel multilayers depends on their thickness. The thickest multilayers show stability up to a temperature of 375 °C. Thinner multilayers exhibit stability up to a higher temperature of 400 °C, in spite of their thermal expansion coefficients being greater.

**Keywords** Cu/310S multilayers · Temperature stability · Thermal expansion coefficients · X-ray diffractometry (XRD)

## 1 Introduction

The term temperature stability is used to define material state changes, or their absence, as a function of temperature and its action time. The so-called temperature stability can be considered with reference to both the structure of material and its physical or mechanical properties. Annealing at elevated temperatures may lead to nucleation and crystallite growth, stress relaxation and mutual diffusion of compounds, both in amorphous and in crystalline materials. The nature of occurring structural changes

---

✉ Edyta Olejnik  
e17dyta@interia.eu

Barbara Kucharska  
kucharska.barbara@wip.pcz.pl

<sup>1</sup> Institute of Materials Engineering, Faculty of Processing Engineering and Materials Technology, Czestochowa University of Technology, Czestochowa, Poland

<sup>2</sup> Welding Laboratory, Gamma Montex, Czestochowa, Poland

depends on both annealing temperature and initial material state [1–4]. For example, the studies of nanostructures and nanometric multilayers have shown that the crystallite growth occurs at lower temperatures, compared to microcrystalline materials [1, 5].

In massive, bulky materials, annealing is used also to either homogenize or recrystallize the material (at a relatively higher temperature) and to minimize stresses introduced to the material with technological operations, such as stress relief treatment (at a relatively lower temperature). In such instances, annealing, through some changes in the material structure, leads to the material attaining a state close to an equilibrium and stress-free one.

Quite the contrary, in the case of coatings and surface layers operating at elevated temperatures this may result in the generation of stresses due to differences in thermal expansion between the layer or coating material and the substrate. The physical temperature stability of coatings will depend also on the type of its bonding with the substrate (e.g., adhesion, diffusion). In the cases of the prolonged action of elevated temperature and the occurrence of diffusion phenomena, the nature of bonding with the substrate may change [6–9]. The most commonly used substrate for thin film components in microelectronics is monocrystalline silicon. As a semiconductor, it is characterized by a large heat capacity [10, 11].

A special case of thin coatings (films) are multilayer systems of nanometric thicknesses, so-called supernets [12, 13]. It is such layered systems that contemporary microelectronics and optoelectronics rely on [14]. Multilayers exhibit unique magnetic properties owing to a large share of interfaces in the multilayer volume [15–17]. For example, classic multilayers built of alternate ferromagnetic and diamagnetic material layers, such Cu/Ni, have been used as high magnetoresistance parts in electronic devices used for magnetic recording. Their functional, magnetic and mechanical properties result from and depend on the period of the layered structure and the state of interfaces [18–22]. It is essential that the interfaces are distinct and have low roughness [23–26]. From among the methods of manufacturing multilayered systems, the most effective in this respect seems to be the magnetron sputtering method, which ensures a uniform thickness of the layers and their good packing [12, 15, 27–30], better than those produced by the electrochemical method [31]. Multilayered systems show a hardness level much higher than that of their individual components. This is explained by a large number of interfaces in them and the misfit of their component lattice parameters and, if they are made by PVD techniques, also by their columnar structure [19–22, 24]. Thus, they impart added anti-wear or sliding properties to the material surface, enabling thereby the multilayers to be applied in electronics and in other areas.

In the conditions of the actual operation of an electronic part with a film on its surface and the potential risk of, e.g., a strong electric impulse occurring periodically, or the need for mounting the part (e.g., by soldering of M-RAM memory), the supplied thermal energy might cause mutual diffusion between the sublayer components [32, 33]. As a consequence, this will result in a change in their physical (a disappearance of magnetic properties) [34, 35] and mechanical (a reduction in hardness) characteristics due to a blurring of the interfaces [36–38].

In the work [39] concerning Cu/Ni multilayers produced by the PVD technique in an ultra-high vacuum, it was demonstrated that annealing of those multilayers for

15 min at a temperature of merely 50 °C has widened the interfaces. It has also been shown that one-time short-term annealing of such multilayers at a higher temperature (500 °C/2 min) may improve their mechanical properties, which is attributed to a reduction in interface roughness, or regrouping of atoms due to the supplied energy and reducing the number of defects in the interface region [40]. Stresses are generated by a lattice misfit, and this depends both on the components used for making the multilayer, and on its thickness (number of sublayers) and the substrate. The same conclusions are drawn from diffusion modeling in multilayer systems [33, 41]. In turn, AES examinations showed that annealing Cu/Ni multilayers (325–375 °C for 30 min.) caused a mutual diffusion of the components only at the interface closest to the silicon substrate [42].

The present study describes investigation into the temperature stability of Cu/Ni-type multilayers, in which Ni was substituted with sublayers with the chemical composition of heat-resistant chromium–nickel stainless steel 310S. Considering the fact that mutual diffusion runs slower in the Cu–FeCrNi system than in the Cu/Ni system [43, 44], it was assumed that the temperature stability of multilayers with a steel sublayer could be better.

Chromium–nickel stainless steels (series AISI 300) made in traditional technology have an austenite structure (fcc, non-magnetic) due to Ni contained in them in a concentration above 10 wt%. In the conditions of sputtering in PVD processes and depositing them as a coating, the structure of these steels can be either type fcc, or wholly or partially type bcc [45–47]. Studies concerning Cu/steel 304 (approx. 18 wt% of Ni) multilayers have shown that the steel layers have an fcc structure, when their thickness does not exceed 5 nm, while in the case of thicker layers, a bcc structure forms [39]. Investigations of PVD 310S steel coatings with a higher (approx. 25 %) content of austenite-stabilizing Ni have found that their structure can also be entirely type bcc. The non-equilibrium bcc phase undergoes transition into the equilibrium fcc phase at a temperature of about 500 °C [48].

Within the present study, multilayers were investigated in a temperature interval of up to 400 °C. The novelty of the presented investigations consists in the use of steel 310S in multilayers, which is similar to superalloys, and has a higher Ni concentration and a better heat resistance compared to steel 304, with which multilayers have already been studied by Zhang [4, 39]. Studies of multilayers with heat-resistant steels can lead to their application in the conditions of elevated temperature, e.g., in magnetic field sensors.

## 2 Material

Multilayers fabricated with the PVD magnetron sputtering technique in a vacuum device equipped with two magnetrons and a rotary table/diaphragm for mounting coating substrates (Fig. 1a) were examined [49].

Targets Ø110 mm of pure copper and of AISI310S (X8CrNi25–21, 1.4548) chromium–nickel steel of chemical composition as shown in Table 1 were mounted on the magnetrons.

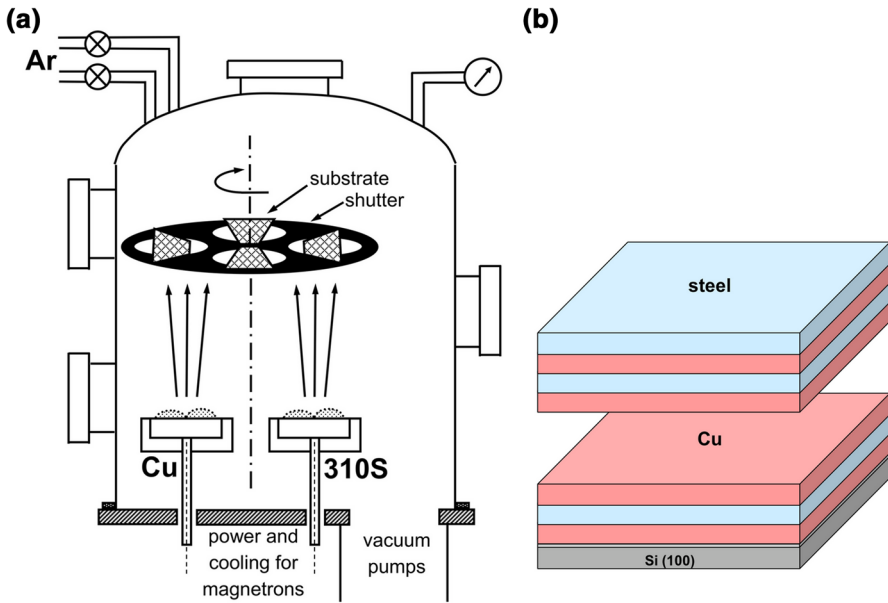


**Fig. 1** (a) Schematic diagram of the vacuum chamber and (b) the structure of the examined multilayer

**Table 1** Chemical composition of AISI310S steel, wt%

| C     | Si    | Mn   | Cr    | Ni    | P      | S      | N     | Fe  |
|-------|-------|------|-------|-------|--------|--------|-------|-----|
| ≤0.10 | ≤1.50 | ≤2.0 | 24–26 | 19–22 | ≤0.045 | ≤0.015 | ≤0.11 | ~50 |

The sputtering process was conducted at an argon pressure of  $2 \times 10^{-3}$  Torr. Multilayers were deposited unilaterally on a monocrystalline silicon Si(100) substrate of dimensions of  $12 \times 12$  mm, subjected to the standard procedure of cleaning the substrates in glow discharge plasma in vacuum chamber.

The multilayers were composed of two repeated bilayers of copper and steel, respectively. The number of bilayers in the multilayers was 50, 100 and 150. The thickness of Cu bilayers was identical in all examined multilayers, amounting to 2 nm, while the thickness of steel bilayers was 2 nm and 4 nm (Fig. 1b). The thickness of individual layers was controlled by magnetron power and deposition time. The power of the magnetron with a Cu target was 500 W, which yielded a power density of  $\sim 7 \text{ W}\cdot\text{cm}^{-2}$ . The power of the magnetron with a 310S steel target was 1600 W and 3200 W, which gave a power density of  $\sim 20 \text{ W}\cdot\text{cm}^{-2}$  and  $\sim 40 \text{ W}\cdot\text{cm}^{-2}$ , respectively.

### 3 Methodology

Multilayer temperature stability tests were performed in an air atmosphere by isothermal annealing in the temperature range from 23 °C to 400 °C. Multilayer annealing was carried out in two stages:

- in the temperature range from 23 °C to 200 °C in the diffractometer chamber (at each temperature duration of annealing cycles was 30 min). The measurements in the diffractometer chamber were carried out using a temperature attachment made to the authors' design, having an automatic controller and a temperature readout capability [50]. Heating of specimens with coatings was effected from the bottom, on the substrate side, while XRD measurements were taken on the coating surface side;
- in the temperature range from 225 °C to 400 °C in an laboratory oven (at each temperature duration of annealing cycles was 15 min). Diffractometric measurements were taken each time after taking out the specimens from the oven and cooling them down to ambient temperature.

XRD measurements were done using diffractometers in symmetric Bragg–Brentano geometry: a Seifert 3003TT with a cobalt anode ( $K_{\alpha}\text{Co} = 0.17\ 903\ \text{nm}$ ) tube in the diffraction angle range of  $2\Theta = 43^{\circ}\text{--}58^{\circ}$  and  $2\Theta = 25^{\circ}\text{--}120^{\circ}$  for annealed multilayers and a high-resolution XPertMPD with a copper anode ( $K_{\alpha}\text{Cu} = 0.15\ 418\ \text{nm}$ ) for multilayers in an as-deposited state. After successive annealing cycles, the surface condition of multilayers was examined using a Zeiss Neophot 32 light microscope.

## 4 Investigation Results

### 4.1 Bilayer Thickness

The multilayered structure of the Cu/310S systems fabricated by the PVD method was confirmed in X-ray examinations. A zero reflection from the multilayer material [ML, Cu/310S (111)] at angles of about  $2\Theta_{\text{Cu}} = 43.37^{\circ}$  and  $43.42^{\circ}$  ( $d_{\text{hkl}} = 0.2086\ \text{nm}$  0.2083 nm), respectively, for Cu/310S = 2/2 nm and Cu/310S = 2/4 nm multilayers, and satellite reflections,  $S_{-1}$  and  $S_{+1}$  were recorded on the diffraction patterns (Fig. 2).

The best representation of the satellite reflections was obtained for multilayers with the largest number of periods, so with the greatest number of interfaces.

In multilayers of the assumed thicknesses 2/2 nm, the satellite reflections did not revealed themselves symmetrically on either side of the main Cu/310S(111) reflection. The satellite reflection  $S_{-1}$  showed up better in all multilayers. The reflection  $S_{+1}$  emerged in multilayers with a thicker steel sublayer (2/4 nm). The poor emergence of satellite reflections is usually associated either with a poor quality of interfaces (high roughness) or with similar lattice parameters of phases making up the sublayers. In such instances, the intensity of satellite reflections is very low, compared to the zero reflection, and often it is impossible to disclose them. The phases in the fabricated multilayers in an equilibrium state are characterized by the following lattice parameters:

- copper (fcc):  $a_{\text{Cu}} = 0.3615\ \text{nm}$ ,  $d_{\text{Cu}}^{111} = 0.2088\ \text{nm}$ ,  
in turn, the steel layer, depending on the structure
- $\gamma$  iron (fcc):  $a_{\text{Fe}\gamma} = 0.3600\ \text{nm}$ ,  $d_{\text{Fe}\gamma}^{111} = 0.2080\ \text{nm}$

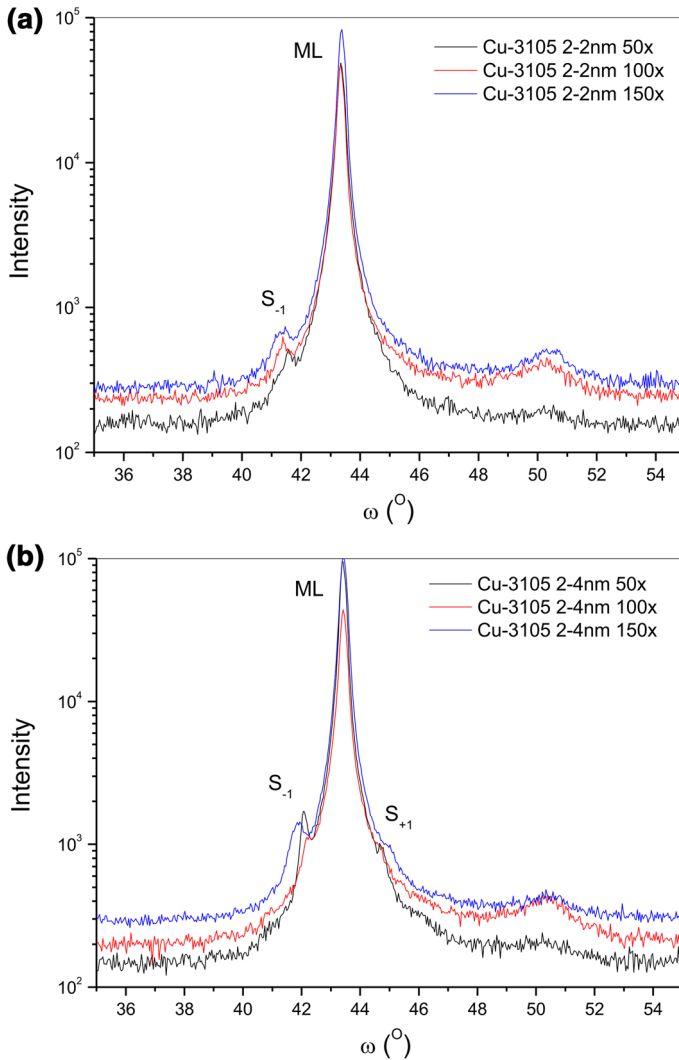


**Fig. 2** Multilayer diffraction patterns (a) Cu/steel = 2/2 nm and (b) Cu/steel = 2/4 nm ( $K_{\alpha}$ Co)

- $\alpha$  iron (bcc):  $a_{\text{Fe}\alpha} = 0.2866$  nm,  $d_{\text{Fe}\alpha}^{110} = 0.2027$  nm.

Copper and  $\gamma$  iron have very similar parameters; if  $\alpha$  iron forms, the representation of satellite peaks in the diffraction patterns should theoretically be better. With the PVD process parameters used, the steel sublayers had an fcc structure ( $a = 0.3591$  nm), as determined by X-ray examination of a control layer deposited also on an Si substrate (Fig. 3).

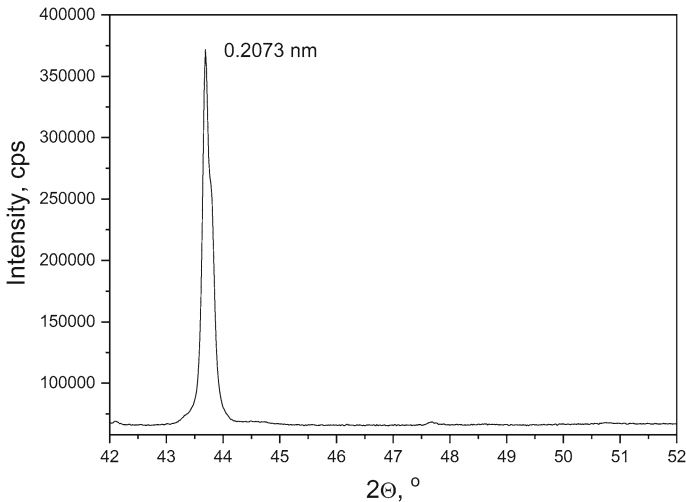


**Fig. 3** Diffraction pattern ( $K_{\alpha}$ Cu) of layer from sputtered 310S steel

To determine the thickness of the period (bilayers) in the examined multilayers, we made use of the position of the zero reflection and one satellite reflection, based on Eq. (1).

$$\Lambda = \lambda / 2(\sin \Theta_i - \sin \Theta_n) \quad (1)$$

where  $i$ —main peak from the lattice plane;  $n$ —satellite peak  $S_{-1}$  associated with the main peak;  $\Lambda$ —period thickness, nm;  $\lambda$ —X-ray radiation wavelength, nm.

The determined thicknesses of bilayers in the fabricated multilayers deviated slightly from those assumed in the PVD deposition process (Table 2). The closest to the assumed thicknesses were multilayers with the largest number of bilayers. In other multilayers, the periods were greater, especially in the multilayer Cu/310S = 2/4 nm 100× (with 1.9 nm—32 %) and in the multilayer Cu/310S = 2/2 nm 50× (with 1.5 nm—37 %). Multilayers with a comparable layer thickness had greater lattice parameters (0.3611–0.3614 nm), similar to the parameters of copper. Multilayers with a thicker steel sublayer that is with a larger steel fraction of the multilayer volume had lattice parameters (0.3607–0.3608 nm) similar to those of steel.

#### 4.2 *In Situ* Measurements at a Temperature of 23–200 °C

Multilayer diffraction patterns ( $K_{\alpha}$ Co) recorded at a annealing temperature increased successively every 30–40 °C are shown in Figs. 4, 5 and 6. The diffraction patterns were also recorded during cooling the multilayers down to ambient temperature.

The *in situ* measurements found that with the increase in multilayer annealing temperature, the angular position of the main reflection, well as the satellite peaks, shifted toward smaller diffraction angles due to a gradual increase in the lattice parameter of the multilayer components. The changes in lattice parameter  $a$ , determined based on

**Table 2** Types and thicknesses of sublayers in the fabricated Cu/310S steel multilayers

| Number of bilayers | Technological assumptions         |                                     |                | Fabricated  |                                  |   |
|--------------------|-----------------------------------|-------------------------------------|----------------|---|----------------------------------|---|
|                    | Thickness of the Cu sublayer (nm) | Thickness of the 310S sublayer (nm) | $\Lambda$ (nm) | $\Lambda$ determined by XRD ( $K_{\alpha}$ Cu) (nm) | Thickness of the multilayer (nm) | Lattice parameter $a$ , determined by XRD ( $K_{\alpha}$ Cu) (nm) |
| 50                 | 2                                 | 2                                   | 4              | 5.5   | 275                              | 0.36 135  |
|                    |                                   | 4                                   | 6              | 7.0   | 350                              | 0.36 083  |
| 100                | 2                                 | 2                                   | 4              | 4.9   | 490                              | 0.36 141  |
|                    |                                   | 4                                   | 6              | 7.9   | 790                              | 0.36 073  |
| 150                | 2                                 | 2                                   | 4              | 4.6   | 690                              | 0.36 114  |
|                    |                                   | 4                                   | 6              | 6.0   | 900                              | 0.36 071  |

the main reflection, during heating and during cooling of the multilayers are illustrated in Fig. 5.

The lattice parameters increased linearly with increasing temperature. The linear regression of parameters  $a$  as a function of heating temperature up to 200 °C (Table 3) enabled the determination of the thermal expansion coefficients  $\alpha$  of multilayers from formula (2).

$$\alpha = (a^T - a_o)/a_o \cdot \Delta T \quad (2)$$

where  $\alpha$ —coefficient of linear expansion,  $K^{-1}$ ,  $a^T$ —lattice parameter determined at temperature  $T$ , Å,  $a_o$ —lattice parameter determined at ambient temperature, Å,  $\Delta T$ —difference between the measurement temperature and ambient temperature,  $K^{-1}$ .

The calculated thermal expansion coefficients, like the lattice parameters, were smaller for multilayers with a thicker 310S steel sublayer. Multilayers with a comparable Cu sublayer and 310S steel sublayer had larger lattice parameters and exhibited a greater expansion (Fig. 6).

So, the both parameters showed a dependence on the component volumetric fraction of the multilayer. While for the lattice parameter, this dependence is obvious—a larger fraction of steel with a smaller lattice parameter caused a smaller parameter of the multilayer, this is no longer so for the expansion. The thermal expansion coefficients  $\alpha$  of the components used for multilayer fabrication, which is copper and 310S steel, were identical. Cu and austenitic steel in a temperature range of up to 200 °C both have a coefficient of  $1.65 \times 10^{-5}/^{\circ}C$  (for sputtered 310S steel with thickness 8  $\mu m$  we found expansion  $1.51 \times 10^{-5}/^{\circ}C$  [51]); hence, it could be expected that the fraction of individual phases of the multilayer would not influence the coefficient value. The value of the thermal expansion coefficient was dependent on the total multilayer thickness—the greater the multilayered system thickness, the smaller the expansion.



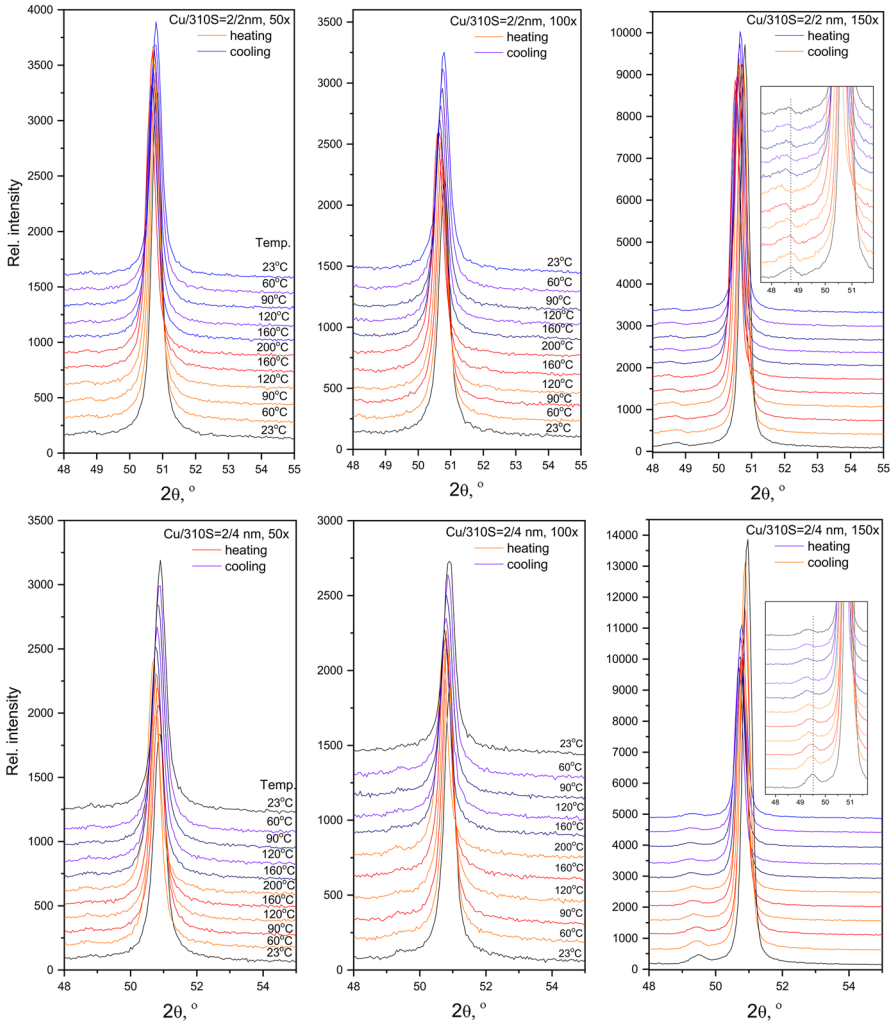


**Fig. 4** Diffraction patterns recorded *in situ* for multilayers annealed at a temperature varying up to 200 °C and then cooled down

In the case of multilayers, in which sublayer components have different thermal expansion coefficients, the overall expansion of the multilayer depends on the volumetric fraction (thickness) of individual sublayers. Figure 6 shows additionally the value of the thermal expansion of Cu/Ni multilayers examined by the authors under the same apparatus conditions, as described in work [52]. The value of  $\alpha$  for Ni is  $1.34 \times 10^{-5}/^{\circ}\text{C}$ ; therefore, the Cu/Ni multilayer had a smaller coefficient than the Cu/310S multilayer with the identical number of bilayers with comparable thicknesses.

Based on the measurements taken, the calculation of the thermal expansion coefficients was also made for narrower temperature ranges (23 °C–T, where T < 200 °C), as illustrated in Fig. 7. They show that in the temperature ranges where the maximum

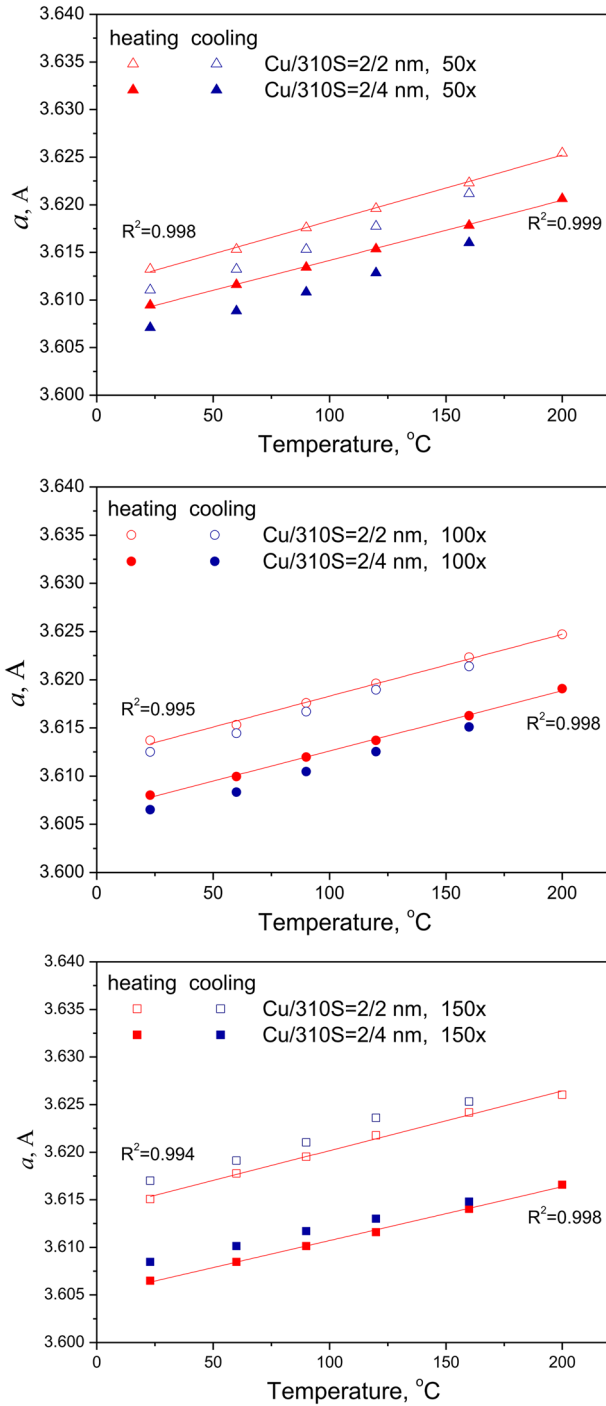
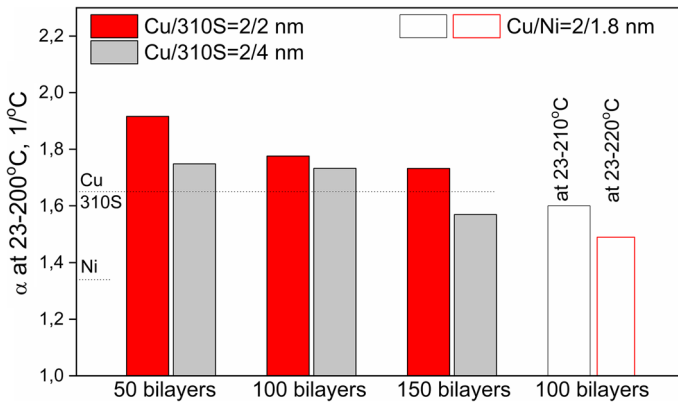


Fig. 5 Lattice parameter of multilayers at varying temperatures during heating and during cooling



**Fig. 6** Thermal expansion coefficients of Cu/310S multilayers in the temperature range of 23–200 °C. Posts that are not filled with color represent the thermal expansion of multilayers Cu/Ni = 2/1.8 nm determined by the authors at work [53]. The broken line illustrates the value of α for solid copper, 310S steel and Ni (Color figure online)

**Table 3** Results of the linear regression of lattice parameter *a* as a function of heating temperature

| Multilayers |     | Slope, $\Delta a/\Delta T$<br>( $\text{Å}\cdot\text{°C}^{-1}$ ) | Intercept, <i>a</i> (Å) | <i>a</i> at 23 °C (Å) |
|-------------|-----|---|-------------------------|-----------------------|
| 50×         | 2/2 | $6.9226 \times 10^{-5}$   | 3.6114                  | 3.6130                |
|             | 2/4 | $6.3098 \times 10^{-5}$   | 3.6079                  | 3.6093                |
| 100×        | 2/2 | $6.4174 \times 10^{-5}$   | 3.6119                  | 3.6134                |
|             | 2/4 | $6.2494 \times 10^{-5}$   | 3.6064                  | 3.6078                |
| 150×        | 2/2 | $6.2609 \times 10^{-5}$   | 3.6139                  | 3.6153                |
|             | 2/4 | $5.6615 \times 10^{-5}$   | 3.6051                  | 3.6064                |

temperature value does not exceed 120 °C, the α coefficients assumed values deviating from those determined for the range of 23–200 °C, especially in the case of thinner multilayers.

After cooling the multilayers from the temperature 200 °C to room temperature, the main reflections of the multilayers returned to higher diffraction angles. Their positions, however, were slightly shifted relative to the reflections recorded during heating, which, apart from thermal dilatation, may also mean the occurrence of diffusion processes within the multilayer. First signs of a mutual diffusion between the components of multilayers were first observed during annealing of the multilayers in 160 °C, which was demonstrated by lower intensity of satellite peaks (Fig. 4). The value of the thermal expansion coefficients obtained by means of diffraction measurements in temperatures ranging from 160 °C and higher, may be flawed due to a mutual diffusion of the components.

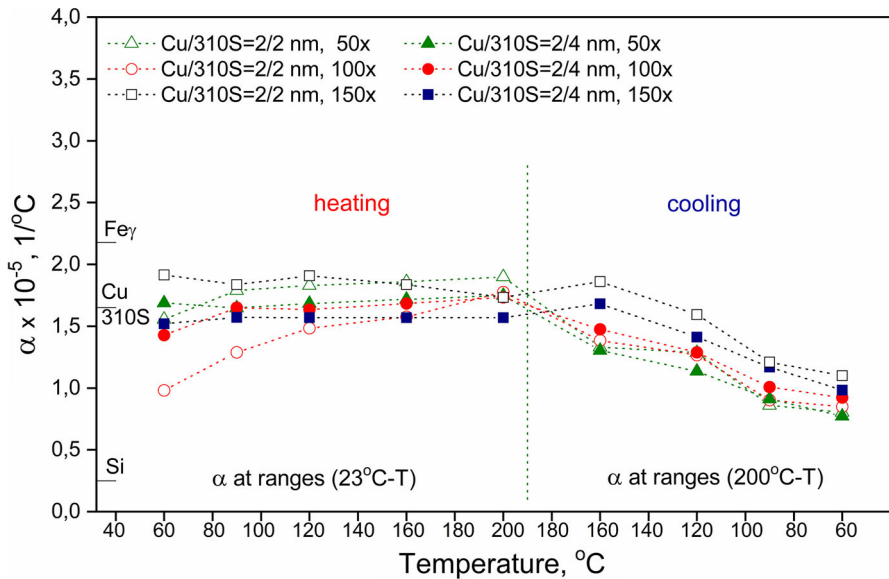


**Fig. 7** Thermal expansion coefficients of Cu/310S multilayers. Each point in the diagram indicates a thermal expansion coefficient value in a different temperature range, from ambient temperature  $T_{\text{otocz}}$  to measurement temperature  $T$

#### 4.3 Measurements After Annealing at a Temperature of 225–400 °C

Diffraction patterns recorded for multilayers annealed at a temperature higher than 200 °C and then cooled down to ambient temperature are shown in Fig. 8. Figure 9 compares the intensities and angular positions of all recorded diffraction patterns, including those obtained from *in situ* measurements. The comparison shows that the intensity of the main reflection from multilayers built of 50 and 100 bilayers stayed at a similar level in all measurement cases. By contrast, the intensity of the reflection from multilayers built of 150 bilayers decreased with annealing temperature and time, regardless of whether the measurement was taken at the annealing temperature or after cooling down to ambient temperature. This means that the thickest multilayers built of 150 bilayers were characterized by a strong texture of planes (111), as confirmed by the diffraction patterns in Fig. 4. This texture vanished as a result of annealing. Hence, the recorded drop in reflection intensity was not affected by whether the measurement was taken at the annealing temperature or after cooling the multilayer down to ambient temperature. The reduction in the intensity of the main reflection from the thickest multilayers occurred to a annealing temperature of 300 °C, after which the intensity stabilized (Fig. 9a). The changes in the intensity of reflections were accompanied by increasing of their half-width (Fig. 9b). An increasing reflection width may result from the formation of “solution” regions in multilayers due to mutual diffusion of their components.

In addition, comparison was made of the angular position of the main reflection of multilayers during annealing them at a temperature of 200 °C and after annealing and

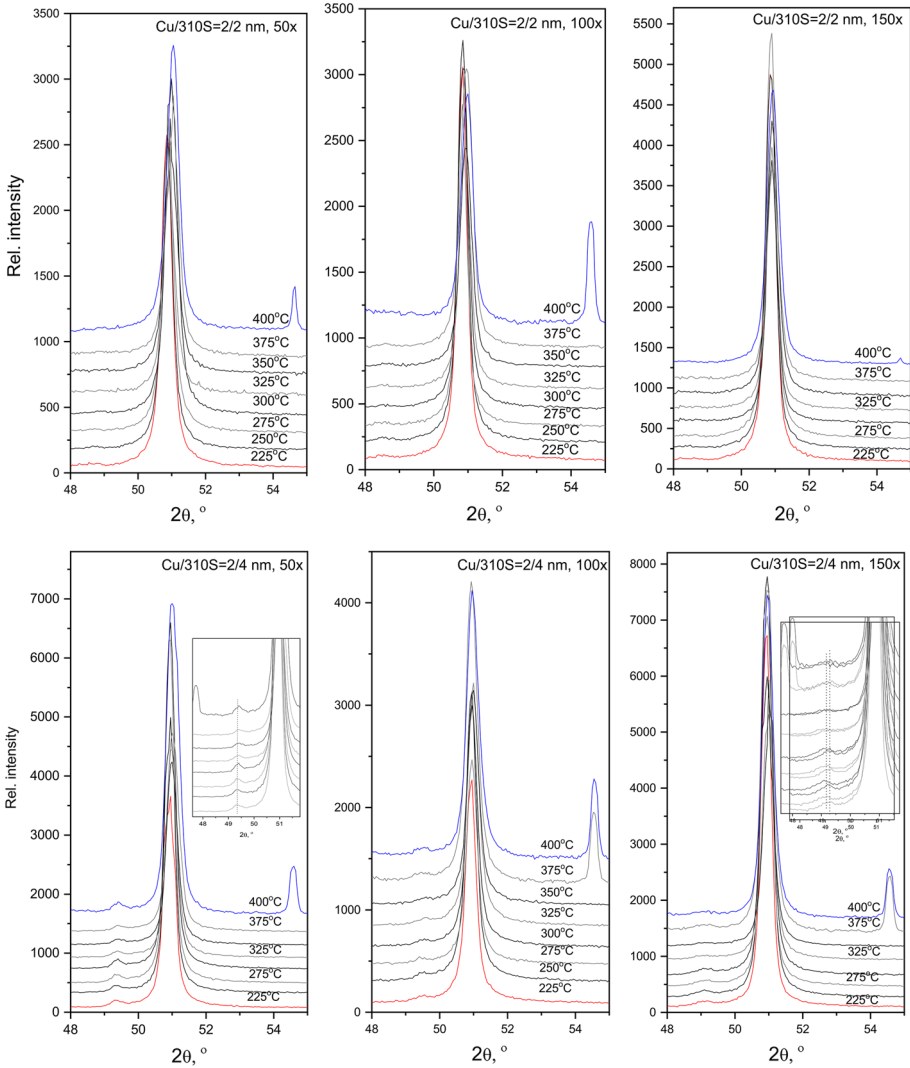


**Fig. 8** Diffraction patterns of multilayers annealed at a temperature varying up to 400 °C and then cooled down

cooling down from a higher temperature (Fig. 10). It was found that after being cooled down from 200 °C, the reflections were slightly shifted toward smaller  $2\Theta$  angles relative to their position prior to annealing, while after being cooled down from 400 °C, slightly shifter toward greater  $2\Theta$  angles. For the case of annealing at 200 °C, such changes can be associated with a decrease in the level of stress introduced during deposition in the PVD process. For annealing at 400 °C, taking additionally into account the increase in FWHM, they suggest the formation of solution regions and an overall reduction in the lattice parameter. A confirmation of diffusion phenomena occurring

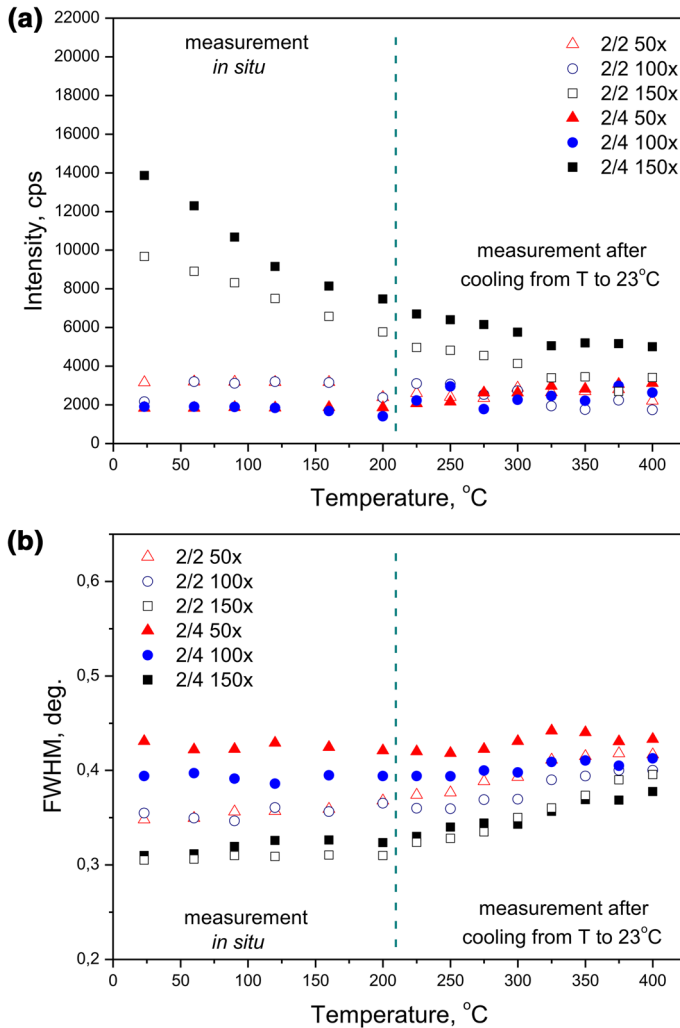


**Fig. 9** Change in the intensity (a) and FWHM (b) of the (111) reflection in *in situ* measurements and after cooling down to ambient temperature

in multilayers is also the changes in the satellite peaks. As annealing progressed, they were reduced in size and widened, which is indicative of interface blurring.

At a temperature of 400 °C and 375 °C, for the thickest multilayers ( $\text{Cu}/310\text{S} = 2/4\ 100\times$  and  $\text{Cu}/310\text{S} = 2/4\ 150\times$ ), additional reflections from the silicon substrate were recorded in the diffraction patterns (Fig. 8). This meant that the multilayers became damaged. The assessment of the multilayer surface condition confirmed the occurrence of brittle multilayer splinters at the edges of the examined specimens (Fig. 11). Figure 11b shows additionally a splinter (splinter) in the central region of the multilayer surface, caused by the gauge of specimen setting in the diffractometer chamber (micrometer end). This implies that the multilayer delamination occurred

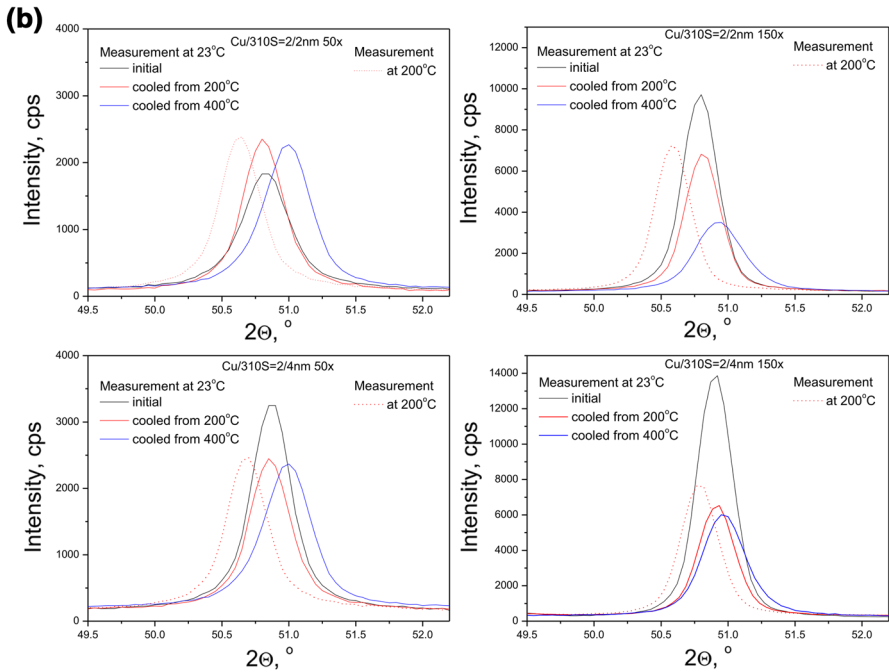
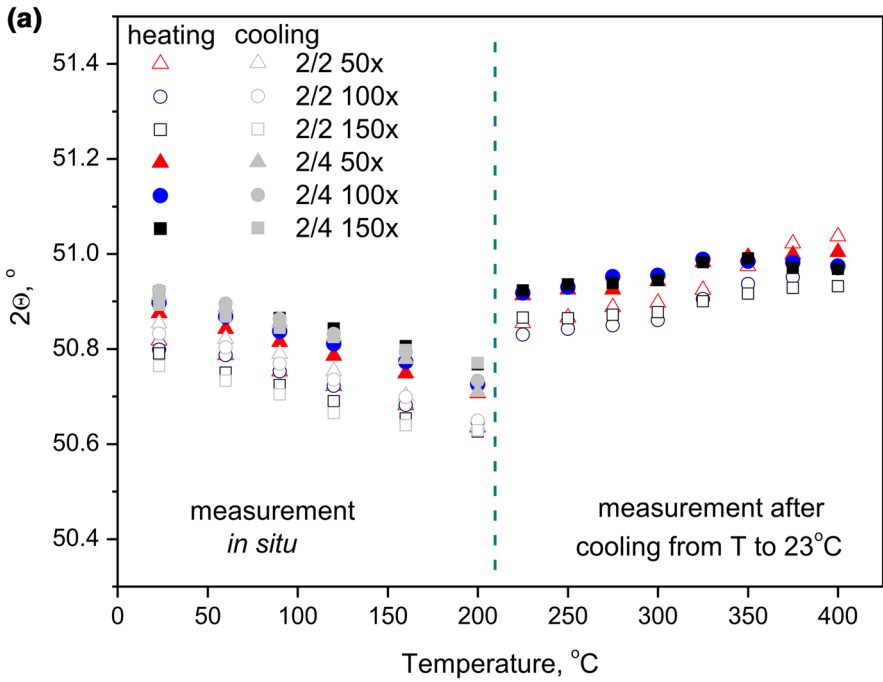


**Fig. 10** (a) Changes in the angular position of the (111) reflection from multilayers in *in situ* measurements and after cooling down to ambient temperature and (b) profiles of selected reflections from the multilayer Cu/310S = 2/2 nm 50x

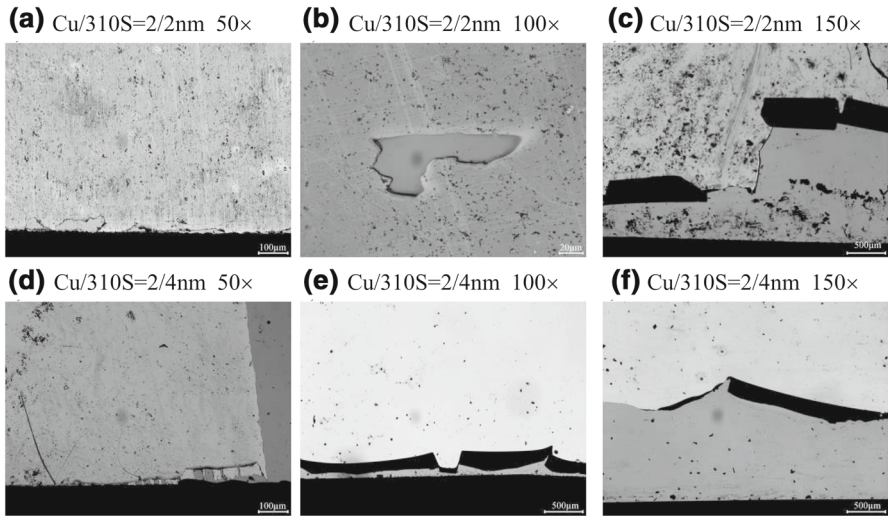


**Fig. 11** Defects in Cu/310S = 2/2 nm multilayers occurred as a result of annealing at 400 °C: (a) Cu/310S = 2/2 nm 50×, (b) Cu/310S = 2/2 nm 100×, (c) Cu/310S = 2/2 nm 150×, (d) Cu/310S = 2/4 nm 50×, (e) Cu/310S = 2/4 nm 100×, (f) Cu/310S = 2/4 nm 150×

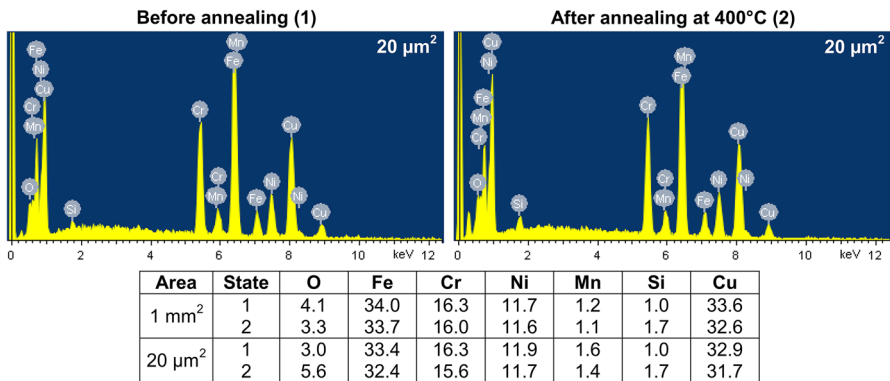


**Fig. 12** Examples EDX spectrum and chemical composition (at.%) of Cu/310S = 2/4 nm multilayers before and after annealing at 400 °C (average values from 2 to 3 analyses)

in a larger area, not only at the edges, and the multilayer itself became brittle. The occurrence of splinters is due to a large difference in thermal expansion coefficients between the silicon substrate and the multilayer components, which caused a disruption of multilayer integrity as a result of stresses occurring at the substrate–multilayer interface. The thermal expansion coefficients of the thickest multilayers were smaller than those of thinner multilayers; nevertheless, it was in these multilayers that the greatest stresses were generated.

On the example of Cu/310S = 2/4 nm multilayer, the chemical composition of its surface was compared before and after annealing at 400 °C. The EDX analysis was performed on areas of approx. 1 mm<sup>2</sup> i 20 µm<sup>2</sup> (Fig. 12).



Even though the analysis of oxygen by this method is only indicative in character, yet it can be taken into consideration in comparative examinations. The comparison shows that the oxygen concentration on the surface of multilayer before and after the heat treatment ranges from 3.0 at.% to 4.1 at.% and from 3.3 at.% to 5.5 at.%, respectively. Such a difference in oxygen concentration, with almost constant ratio of alloying elements in steel, does not clearly indicate a significant increase in the amount of oxides on the surface of the multilayer. It should be emphasized that the outer layer of Cu/310S multilayers, which has a direct contact with the air, was made of steel. The heat resistance of steel is provided by chromium due to a very thin passive layer of  $\text{Cr}_2\text{O}_3$  oxide, which is formed on its surface. This layer was also created on the surface of multilayers, protecting them against further oxidation.

## 5 Discussion

Examinations of the thermal stability of multilayered systems are usually focused on the determination of the state of interfaces and the diffusion of components within them. The state of interfaces is determined by, inter alia, the degree of misfit between the adjacent phases, which generates stress.

When selecting the thickness of the 310S steel sublayer (2 nm and 4 nm) for the multilayers examined within this study, the results published by Zhang et al. [2] relating to Cu/304 multilayers were taken into account. Namely, it has been shown that sublayers of steel 304 (~9 wt% Ni) of a thickness less than 5 nm have an fcc structure. Steel 310S contains more Ni (~20 wt%) that stabilizes the fcc structure; therefore, it meets this criterion even more so, as confirmed in Fig. 4. The degree of lattice misfit between Cu and steel 310S in the multilayer is only 0.4 %. In this study, the thermal stability of the multilayer has been determined chiefly in terms of its retaining adhesion with the silicon substrate. Therefore, this little lattice misfit, with a similar thermal expansion of both phases, allows one to infer a minimization of a possible effect of interfacial stress on the examined stability in the Cu/310S. Indeed, a delamination of the multilayer from its silicon substrate was found, without its own delamination.

In the selection of the test temperature, the results published by Zhang et al. [39] were also considered, which showed that, in Cu/304 multilayers, an interface blurring due to diffusion had occurred after annealing at 550 °C for 1 h. In the present study, lower temperatures (up to 375–400 °C) and shorter annealing durations were applied. Therefore, it could be expected that the interdiffusion of components would be limited. This claim seems to be supported by well-distinguished satellite peaks, especially in diffraction patterns obtained from the thickest multilayers. Based on the above explanations, it seems that, in the investigations carried out, the thermal stability of the Cu/310S multilayers is mostly a consequence of differences in thermal expansion between the substrates and the multilayers and their thickness, with a minimization of the effect of lattice misfit within interfaces and interdiffusion.

Nevertheless, it should be noted that the total multilayer annealing duration (approx. 30 min at each temperature) was longer than that used in study [39]. Therefore, in their further studies, the authors will determine the profiles of element concentrations on the multilayer cross sections.

Referring to the previously tested Cu/Ni multilayers, it can be stated that they were delaminated from the silicon substrate at a temperature lower than the Cu/310S multilayers. Namely, multilayers Cu/Ni = 2/1.8 nm 100× were destroyed at a temperature of 230 °C and Cu/Ni = 2/6 nm 100× at 300 °C [52]. In addition, it should be emphasized that the outer layer of Cu/310S multilayers, which has a direct contact with the air, was made of steel (in the Cu/Ni multilayers referred to for comparison, it was made of Ni). Steel 310S is a heat-resistant steel that is similar to superalloys because of its high nickel content, and can be used for operating at temperatures as high as up to 1050 °C. As a result of contact with air, a passive film of Cr<sub>2</sub>O<sub>3</sub> forms on the surface of steel (while on nickel, of NiO). It can be presumed that after annealing, even at a relatively low temperature of 400 °C, the thickness of the passive film on the outer layer of Cu/310S multilayers will increase. However, the Cr<sub>2</sub>O<sub>3</sub> passive film thickness was so small that it was not recorded either in XRD or GXRDX examinations (just like, using these methods, it was impossible to identify NiO oxides on the previously examined Cu/Ni multilayers), as well as in SEM–EDX analysis. On the nanocrystalline structure of a multilayer, also nanocrystalline form, therefore, using high-resolution methods for their observation and analysis is necessary. In addition to the protection of the surface against fast oxidation, a passive film built of Cr<sub>2</sub>O<sub>3</sub> oxides has also a smaller thermal expansion compared to a metallic multilayer; so, it should have a favorable effect on the thermal stability of the multilayer (e.g., in work [53]; an improvement in the thermal stability of the Cu-permalloy (Ni<sub>80</sub>Fe<sub>20</sub>) multilayer was obtained through passivation at the final annealing step at 300 °C/2 h in a controlled forming gas (N<sub>2</sub>–H<sub>2</sub>) atmosphere). The quantity of oxides formed on the surface under the same annealing conditions will be greater on a larger surface area, which is exhibited by multilayers with greater thermal expansion. This could explain why thinner Cu/310S multilayers, with a smaller period thickness and overall thickness, showed better thermal stability.

## 6 Summary

- The examination of multilayers composed of Cu and 310S sublayers, fabricated by the PVD method, has demonstrated a relationship between the multilayer lattice parameter and the volumetric fraction of individual phases of the multilayer. Multilayers with similar thicknesses of Cu and steel sublayers, being equal to 2 nm, had a smaller lattice parameter of 0.36 130–0.36 153 nm (similar to the lattice parameter of Cu), compared to multilayers with a sublayer thickness of, respectively, 2 nm and 4 nm, in which the lattice parameter was 0.36 064–0.36 093 nm.
- The thermal expansion of multilayers in the temperature range of 23–200 °C decreases with increasing steel sublayer thickness and overall multilayer thickness. Cu/310S = 2/2 nm multilayers exhibited thermal expansion in the magnitude range of 1.7318–1.9160 1/°C, that is higher compared to copper and conventional 310S steel, whereas Cu/310S = 2/4 nm multilayers showed thermal expansion in the range of 1.5699–1.7482 1/°C. Multilayers with 50 bilayers had thermal expansion greater by approx. 0.2 1/°C compared to multilayers with 150 bilayers.

- The degree of multilayer texturing increases with increasing multilayer thickness. The texture of planes (111) becomes weakened during annealing in the temperature range of 50–300 °C.
- Annealing of multilayers in the temperature range of 200–400 °C causes a blurring of interfaces due to the mutual diffusion of components. After annealing, the multilayer lattice parameter has decreased, the satellite reflections have widened, and in the thickest multilayers, the half-width of the main reflection has increased, indicating the formation of a solution.
- The temperature stability of Cu/310S steel multilayers deposited on the monocrystalline Si substrate depends on their thickness. The thickest multilayers with a Cu and steel sublayer thickness of, respectively, 2 nm and 4 nm and with the number of bilayers of 100 and 150 show stability up to a temperature of 375 °C. Thinner multilayers exhibit stability up to a higher temperature of 400 °C, in spite of their thermal expansion coefficients being greater.

Comparison of the results of these and the previous investigations shows that the temperature stability of Cu/310S steel multilayers deposited on a monocrystalline silicon substrate is better compared to that of Cu/Ni multilayers with the same number of bilayers with a comparable thickness and deposited on the same substrate.

**Acknowledgment** This work was supported by the Polish National Science Centre (Agreement No. UMO-2012/05/N/ST8/02269).

**Open Access** This article is distributed under the terms of the Creative Commons Attribution 4.0 International License (<http://creativecommons.org/licenses/by/4.0/>), which permits unrestricted use, distribution, and reproduction in any medium, provided you give appropriate credit to the original author(s) and the source, provide a link to the Creative Commons license, and indicate if changes were made.

## References

1. R.A. Andrievski, *J. Mater. Sci.* **38**, 1367–1375 (2003)
2. H.R. Peng, M.M. Gong, Y.Z. Chen, F. Liu, *Int. Mater. Rev.* **62**, 303–333 (2017)
3. I.K. Schuller, *Phys. Rev. Lett.* **44**, 1597–1600 (1980)
4. X. Zhang, A. Misra, H. Wang, H. Kung, J.D. Embursy, R.G. Hoagland, M. Nastasi, *Mater. Res. Soc.* **740**, 49–54 (2003)
5. S. Ganapathi, D.M. Owen, A.H. Chokshi, *Scr. Metall. Mater.* **25**, 2699–2704 (1991)
6. A. Schaub, P. Slepíčka, I. Kašpárková, P. Malinský, A. Macková, V. Švorčík, *Nanoscale Res. Lett.* **8**, 249–257 (2013)
7. O.H. Kessler, F.T. Hoffmann, P. Mayr, *Surf. Coat. Technol.* **108–109**, 211–216 (1998)
8. D. Alontseva, A. Krasavin, T. Kolesnikova, A. Russakova, *Acta Phys. Pol., A* **125**, 1275–1279 (2014)
9. A. Lahmar, T. Nguyen, D. Sackami, S. Orain, Y. Scudeller, F. Danes, *Thin Solid Films* **389**, 167–172 (2001)
10. H. Ernst, E. Müller, W.W. Kaysser, *Microelectron. Reliab.* **40**, 1683–1688 (2000)
11. F.J. Morin, J.P. Maita, *Phys. Rev.* **96**, 28 (1954)
12. M. Stueber, H. Holleck, H. Leiste, K. Seemann, S. Ulrich, C. Ziebert, *J. Alloy. Compd.* **483**, 321–333 (2009)
13. S.A. Barnett, M. Shinn, *Ann. Rev. Mater. Sci.* **24**, 481–511 (1994)
14. A. Thetford, *Opt. Laser Technol.* **3**, 131–135 (1971)
15. F. Stobiecki, T. Stobiecki, *Acta Phys. Pol., A* **102**, 95–108 (2002)
16. L.L. Hinchey, D.L. Mills, *Phys. Rev. B* **33**, 3329–3343 (1986)
17. T. Shinijo, K. Mibu, *Hyperfine Interact.* **144**, 53–64 (2002)

18. G. Nabiyouni, W. Schwarzacher, J. Cryst. Growth **275**, 1259–1262 (2005)
19. B. Kucharska, E. Kulej, G. Pyka, J. Kanak, T. Stobiecki, Mater. Sci. Pol. **31**, 101–107 (2013)
20. H.C. Barshilia, K.S. Rajam, Surf. Coat. Technol. **155**, 195–202 (2002)
21. E. Kulej, B. Kucharska, J. Kanak, Mater. Eng. **32**, 514–516 (2011)
22. B. Kucharska, E. Kulej, J. Kanak, Solid State Phenom. **163**, 291–294 (2010)
23. X.Y. Zhu, X.J. Liu, R.L. Zong, F. Pan, Mater. Sci. **527**, 1243–1248 (2010)
24. L.G. Parratt, Phys. Rev. **95**, 359–369 (1954)
25. P.M. Anderson, J.S. Carpenter, Scr. Mater. **62**, 325–328 (2010)
26. B. Kucharska, E. Kulej, J. Kanak, Opt. Appl. **29**, 881–888 (2009)
27. V.V. Ustinov, L.N. Romashev, T.P. Krinitsina, E.A. Kravtsov, M.A. Milyaev, A.V. Semerikov, V.A. Tsurin, N.V. Kourtina, J. Magn. Magn. Mater. **240**, 511–513 (2002)
28. P.E. Hovsepian, W.-D. Münz, Vacuum **69**, 27–36 (2002)
29. B.G. Wendler, *Functional Coatings by CVD and PVD Methods* (Printing House of Institute for Sustainable Technologies – National Research Institute in Radom, Copyright by B.G. Wendler, Łódź University of Technology, Łódź, 2011)
30. B. Kucharska, E. Kulej, Arch. Metall. Mater. **55**, 45–51 (2010)
31. F. Stobiecki, B. Szymański, T. Luciński, M. Urbaniak, J. Dubowik, R. Gontarz, Elektronika **41**, 29–32 (2000)
32. B. Gągorowska, M. Duś-Sitek, Arch. Metall. Mater. **53**, 889–917 (2006)
33. Z. Erdelyi, D.L. Beke, J. Mater. Sci. **46**, 6465–6483 (2011)
34. H. Sato, T. Matsudai, W. Abdul-Razzaq, C. Fierz, P.A. Schroeder, J. Phys.: Condens. Matter **6**, 6151–6162 (1994)
35. A. Siritariwat, E.W. Hill, I. Stutt, J.M. Fallon, P.J. Grundy, Sens. Actuators **81**, 40–43 (2000)
36. C.B. Ene, G. Schmitz, R. Kirchheim, A. Hütten, Acta Mater. **53**, 3383–3393 (2005)
37. B. Gągorowska, B. Kucharska, M. Duś-Sitek, A. Tokarz, Mater. Sci. Pol. **26**, 149–155 (2008)
38. B. Kucharska, E. Kulej, A. Wróbel, Opt. Appl. **42**, 725–736 (2012)
39. X. Zhang, R.K. Schulze, H. Wang, A. Misra, J. Appl. Phys. **101**, 124311–124315 (2007)
40. Z. Balogh, M.R. Chellali, G.H. Greiwe, G. Schmitz, Z. Erdélyi, Appl. Phys. Lett. **99**, 181902 (2011)
41. J.-M. Roussel, P. Bellon, Phys. Rev. B **73**, 085403 (2006)
42. X.L. Yan, Y. Liu, H.C. Swart, J.Y. Wang, J.J. Terblans, App. Surf. Sci. **364**, 567–572 (2016)
43. I.V. Belova, G.E. Murch, R. Filipek, M. Danielewski, Acta Mater. **53**, 4613–4622 (2005)
44. S.V. Divinski, F. Hisker, Ch. Herzig, R. Filipek, M. Danielewski, Defects Diffus. Forum **237–240**, 50–61 (2005)
45. X. Zhang, A. Misra, R.K. Schulze, C.J. Wetteland, H. Wang, M. Nastasi, J. Mater. Res. **19**, 1696–1702 (2004)
46. S. Inoue, T. Saeki, H. Uchida, K. Koterazawa, M. Iwasa, Vacuum **66**, 257–261 (2002)
47. B. Kucharska, Inż. Mater. Mater. Eng. **3–4**, 419–421 (2007)
48. B. Kucharska, Mater. Sci. Pol. **26**, 181–188 (2008)
49. W.M. Posadowski, Thin Solid Films **459**, 258–261 (2004)
50. B. Kucharska, Z. Nitkiewicz, Inż. Mater. Mater. Eng. **6**, 1072–1075 (2008)
51. B. Kucharska, Solid State Phenom. **163**, 247–252 (2010)
52. E. Olejnik, B. Kucharska, Inż. Mater. Mater. Eng. **36**, 497–500 (2015)
53. M. Mujika, S. Arana, E. Castaño, M. Tijero, R. Vilares, J.M. Ruano-López, A. Cruz, L. Sainz, J. Berganza, Phys. Status Sol A **205**, 1478–1483 (2008)